

## Pseudo-solid-like behavior of nanocomposite melts

A.D. Drozdov,<sup>1</sup> E.A. Jensen<sup>2</sup> and J. deC. Christiansen<sup>2</sup>

<sup>1</sup> *Danish Technological Institute, Gregersensvej 1,  
DK-2630 Taastrup, Denmark*

<sup>2</sup> *Department of Production, Aalborg University Fibigerstraede 16,  
DK-9220 Aalborg, Denmark*

*Phone: +45 72 20 31 42; Fax: +45 72 20 31 12;  
E-mail: Aleksey.Drozdov@teknologisk.dk*

### Abstract

Observations are reported on nanocomposite melts (low-density polyethylene and polypropylene reinforced with montmorillonite nanoclay at concentrations ranging from 0 to 10 wt.-%) in small-amplitude shear oscillatory tests. A constitutive model is derived for the linear viscoelastic response of a nanocomposite melt, which is treated as an inhomogeneous non-affine network of chains. Given a nanoclay content, the stress–strain relations involve 4 material parameters that are found by fitting the experimental data. The pseudo-solid-like response of nanocomposite melts is associated with formation of a “long-tail” in the distribution of activation energies for sliding of junctions due to jamming of stacks of clay platelets.

**Keywords:** Nanocomposite melt; Pseudo-solid-like response; Linear viscoelasticity; Non-affine network; Constitutive model

### 1. Introduction

This paper is concerned with experimental investigation and constitutive modeling of the pseudo-solid-like response of hybrid nanocomposite melts [polyolefins reinforced with montmorillonite (MMT) nanoclay]. This phenomenon is observed in small-amplitude shear oscillatory tests as a pronounced growth of the storage,  $G'$ , and loss,  $G''$ , moduli with concentration of filler. In the interval of relatively low frequencies  $\omega$  (ranging from 0.1 and 1 rad/s), the moduli  $G'(\omega)$  and  $G''(\omega)$  of a neat polymer melt are expected to be proportional to  $\omega^2$  and  $\omega$ , respectively. Reinforcement of the melt causes evolution

of these dependencies. When concentration of nanoclay reaches 3 to 5 wt.-%, the functions  $G'(\omega)$  and  $G''(\omega)$  become weakly dependent of frequency. This transformation is conventionally referred to as formation of low-frequency plateaus or transition to the pseudo-solid-like behavior (the term “solid-like” is associated with the response of an elastic solid, whose storage modulus is independent of frequency, whereas “pseudo” means that the low-frequency plateaus may be destroyed by severe pre-loading). The storage and loss moduli in the plateau region, as well as the interval of frequencies at which the dynamic moduli remain constant, monotonically grow with concentration of nanofiller in both exfoliated and intercalated systems [1, 2]. Formation of the low-frequency plateaus was reported in nanocomposites melts with polyamide [3, 4], polycarbonate [5], poly( $\epsilon$ -caprolactone) [6], polyethylene [7, 8], polyisoprene [9, 10], polypropylene [2, 11], and polystyrene [12] matrices. In another form of presentation of experimental data [13], the pseudo-solid-like response is revealed as a pronounced increase in the complex viscosity

$$\eta^*(\omega) = \frac{1}{\omega} \left[ (G'(\omega))^2 + (G''(\omega))^2 \right]^{\frac{1}{2}}. \quad (1.1)$$

at low frequencies  $\omega$ .

The following explanations were proposed for this phenomenon: (i) confinement of polymer chains within silicate layers in stacks [6], (ii) frictional interactions between tactoids of irregular shape [14], and (iii) formation of a percolated network by stacks of clay platelets due to their jamming [15]. Not arguing their validity, we emphasize that no quantitative models have been developed, where the above processes play the key role.

The objective of this study is two-fold: (i) to report experimental data in small-amplitude shear oscillatory tests on nanocomposite melts with low-density polyethylene (LDPE) and isotactic polypropylene (iPP) matrices reinforced with MMT nanoclay, and (ii) to derive a constitutive model for the linear viscoelastic behavior of nanocomposite melts and to find adjustable parameters in the stress–strain relations by fitting the observations.

To develop constitutive equations with a relatively small number of material constants, we apply a homogenization concept and treat a nanocomposite melt as an equivalent heterogeneous non-affine permanent network of chains. The heterogeneity reflects (i) inhomogeneity in the distribution of clay platelets and their stacks and (ii) local density fluctuations in the polymer matrix. The non-affinity implies that junctions (entanglement between chains and physical cross-links at the surfaces of nanofiller) slide with respect to their reference positions under deformation. The assumption that the network is permanent means that rearrangement of chains (separation of active strands from their junctions and attachment of dangling chains to the network [16]) is disregarded.

The exposition is organized as follows. Observations in shear oscillatory tests are reported in Section 2. Constitutive equations for a nanocomposite melt are developed in Section 3, where phenomenological relations for material functions are proposed. Adjustable parameters are determined in Section 4 by fitting the experimental data. Section 5 provides a brief discussion of our results. Concluding remarks are formulated in Section 6.

## 2. Experimental procedure

Low-density polyethylene Riblene MR10 (density 0.918 g/cm<sup>3</sup>, melt flow index 20 g/10 min, DSC melting peak 107 °C) was supplied by Polimeri Europa (Italy). Isotactic polypropylene Moplen HP 501L (density 0.9 g/cm<sup>3</sup>, melt flow index 6 g/10 min, DSC melting peak 171 °C) was supplied by Basell Polyolefins (Belgium). Masterbatch 1001E [nanocomposite with polypropylene matrix filled with 40 wt.-% of nanoblend concentrate (organically modified MMT nanoclay)] was purchased from PolyOne Inc. (USA). Pellets were melt blended and compounded by using Buss Kneader system ASV 46 at various proportions by weight. These proportions corresponded to concentrations  $\varphi = 0, 1, 2, 3, 4, 5, 6, 8,$  and 10 wt.-% of nanoclay in LDPE/MMT system and  $\varphi = 0, 3, 4, 5, 6, 7,$  and 10 wt.-% in iPP/MMT nanocomposite. Samples for rheological tests were molded by using injection-molding machine Ferromatic K110/S60-2K.

Rheological tests were conducted by using rheometric mechanical spectrometer Paar Physica MCR 500 in a cone-and-plate configuration with a 25 mm diameter disk, an angle of 2°, and a gap length of 0.05 mm. Experiments were performed at the temperatures  $T = 170$  °C for LDPE/MMT and  $T = 200$  °C for iPP/MMT systems. A fresh specimen was used for each test. Triplicate measurements showed good reproducibility of results.

Small-amplitude shear oscillatory tests were performed in the frequency-sweep mode with an amplitude of 0.05 (which ensured the linear viscoelastic response) and angular frequencies ranging from 0.1 to 100 rad/s. In each test, a sample was equilibrated at the required temperature, and the storage modulus  $G'$  and loss modulus  $G''$  were measured at various frequencies  $\omega$  beginning from the largest one. The experimental data are depicted in Figures 1 and 2 (LDPE/MMT) and Figures 3 and 4 (iPP/MMT) in the form of double-logarithmic plots with  $\log = \log_{10}$ . The following conclusions are drawn from Figures 1–4:

1. Given a concentration of nanoclay  $\varphi$ , the storage and loss moduli monotonically increase with frequency of oscillations. For each  $\varphi$ , the growth of  $G'(\omega)$  is stronger than that of  $G''(\omega)$ .
2. Given an angular frequency  $\omega$ , the dynamic moduli monotonically grow with nanofiller content. The increase is rather modest at high frequencies, and it becomes noticeable at low frequencies. At  $\varphi > 4$  wt.-%, low-frequency plateaus are observed on the graphs  $G'(\omega)$ , whereas no plateau is visible on the curves  $G''(\omega)$ .

## 3. Constitutive equations

A nanocomposite melt is modeled as an incompressible heterogeneous non-affine network of chains. Incompressibility implies that deformation of the network is volume-preserving. Non-affinity means that junctions (entanglements between chains and physical cross-links at the surfaces of clay platelets) slide with respect to their reference positions under deformation. Inhomogeneity of the equivalent network is induced by heterogeneous distribution of clay platelets and density fluctuations in the host matrix.

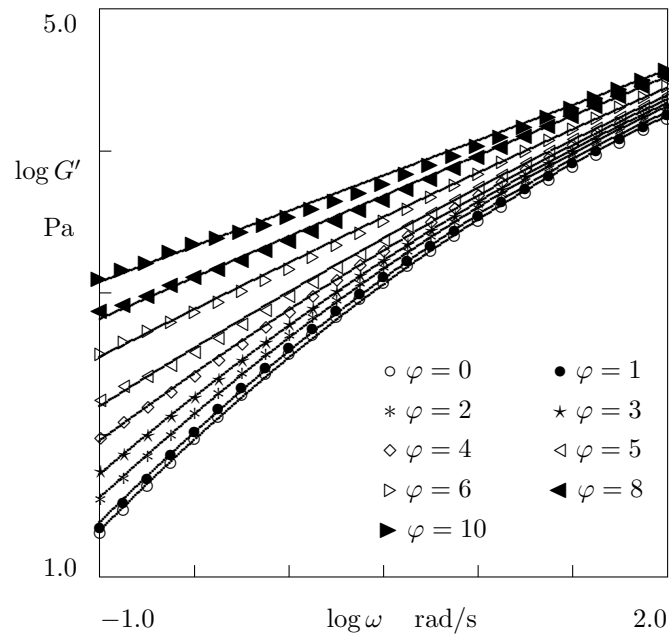


Figure 1: Storage modulus  $G'$  versus frequency  $\omega$ . Symbols: experimental data on LDPE/MMT melts with various concentrations of filler  $\varphi$  wt.-%. Solid lines: results of numerical simulation.

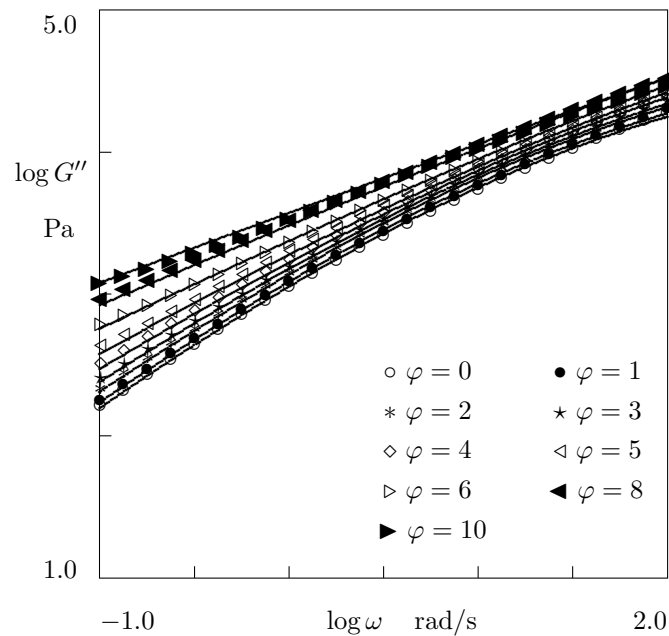


Figure 2: Loss modulus  $G''$  versus frequency  $\omega$ . Symbols: experimental data on LDPE/MMT melts with various concentrations of filler  $\varphi$  wt.-%. Solid lines: results of numerical simulation.

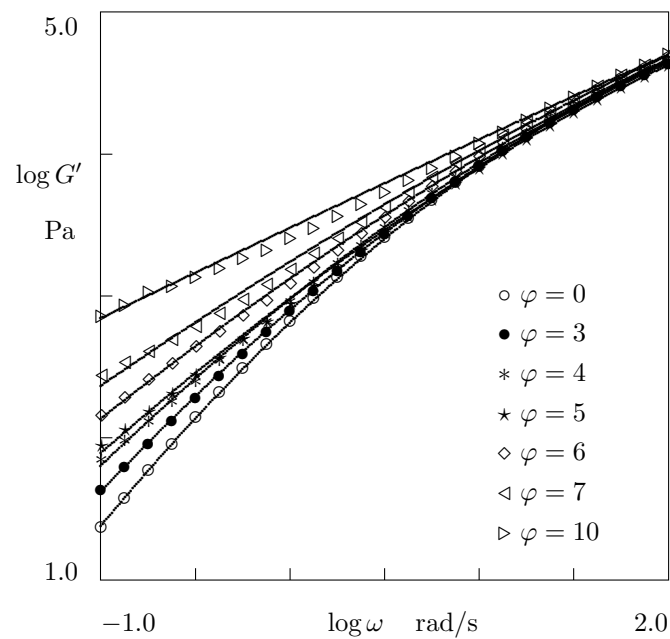


Figure 3: Storage modulus  $G'$  versus frequency  $\omega$ . Symbols: experimental data on iPP/MMT melts with various concentrations of filler  $\varphi$  wt.-%. Solid lines: results of numerical simulation.

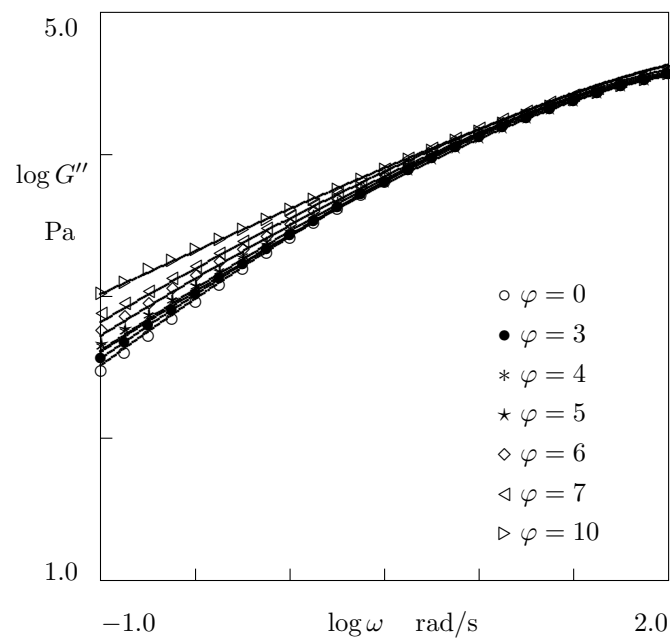


Figure 4: Loss modulus  $G''$  versus frequency  $\omega$ . Symbols: experimental data on iPP/MMT melts with various concentrations of filler  $\varphi$  wt.-%. Solid lines: results of numerical simulation.

To account for this inhomogeneity, a melt is treated as an ensemble of meso-regions, where junctions slide with various rates. These meso-regions may be associated with “mesoscopic domains composed of correlated silicate layers” [3].

Each meso-region is characterized by some energy  $u$ . The rate of sliding of junctions in this meso-region  $\Gamma$  is described by the Eyring equation  $\Gamma = \gamma \exp(-u/(k_B T))$ , where  $T$  stands for absolute temperature,  $k_B$  denotes Boltzmann’s constant, and  $\gamma$  is a constant attempt rate. Introducing the dimensionless energy  $v = u/(k_B T)$ , we present this equality in the form

$$\Gamma(v) = \gamma \exp(-v). \quad (3.1)$$

Inhomogeneity of a nanocomposite melt is characterized by (i) the number  $n(v)$  of chains that belong to meso-regions with dimensionless energy  $v$ , and (ii) the total number of chains  $N = \int_0^\infty n(v)dv$ . The quantities  $n(v)$  and  $N$  are determined per unit volume of the melt. The distribution function of chains is given by

$$f(v) = \frac{n(v)}{N}. \quad (3.2)$$

Macro-deformation of a melt at time  $t \geq 0$  is described by the strain tensor  $\hat{\epsilon}(t)$ , whereas sliding of junctions in a meso-region with energy  $v$  is determined by the strain tensor  $\hat{\epsilon}_s(t, v)$ . At small strains, the strain tensor for elastic deformation reads

$$\hat{\epsilon}_e(t, v) = \hat{\epsilon}(t) - \hat{\epsilon}_s(t, v). \quad (3.3)$$

The strain energy of a chain is determined by

$$w(t, v) = \frac{1}{2} \tilde{\mu} \hat{\epsilon}_e(t, v) : \hat{\epsilon}_e(t, v), \quad (3.4)$$

where  $\tilde{\mu}$  stands for rigidity, and colon denotes convolution of tensors. Disregarding the energy of inter-chain interactions (it is accounted for by means of the incompressibility condition only), we calculate the strain energy per unit volume as the sum of energies of individual chains  $W(t) = \int_0^\infty w(t, v)n(t, v)dv$ . Insertion of Eqs. (3.2) and (3.4) into this equality results in

$$W(t) = \frac{1}{2} \mu \int_0^\infty \hat{\epsilon}_e(t, v) : \hat{\epsilon}_e(t, v) f(v) dv \quad (3.5)$$

with  $\mu = \tilde{\mu} N$ . At isothermal deformation of an incompressible medium, the Clausius–Duhem inequality reads

$$Q(t) = -\frac{dW}{dt}(t) + \hat{\Sigma}'(t) : \frac{d\hat{\epsilon}}{dt}(t) \geq 0,$$

where  $Q$  stands for internal dissipation per unit volume and unit time,  $\hat{\Sigma}$  is the stress tensor, and prime denotes deviator of a tensor. It follows from Eq. (3.5) that the dissipation inequality is satisfied for an arbitrary deformation program, provided that (i) the stress tensor is given by

$$\hat{\Sigma}(t) = -p(t)\hat{I} + \mu \int_0^\infty \hat{\epsilon}_e(t, v) f(v) dv, \quad (3.6)$$

where  $p(t)$  is an unknown pressure, and  $\hat{I}$  is the unit tensor, and (ii) the rate-of strain tensor for sliding of junctions obeys by the equation

$$\frac{\partial \hat{\epsilon}_s}{\partial t}(t, v) = \Gamma(v) \hat{\epsilon}_e(t, v),$$

where  $\Gamma$  is determined by Eq. (3.1). Combination of this equality with Eq. (3.3) results in the differential equation

$$\frac{\partial \hat{\epsilon}_e}{\partial t}(t, v) + \Gamma(v) \hat{\epsilon}_e(t, v) = \frac{d\hat{\epsilon}}{dt}(t). \quad (3.7)$$

The initial condition  $\hat{\epsilon}_e(0, v) = \hat{0}$  for Eq. (3.7) means that the elastic strain vanishes in the reference state.

### 3.1. Adjustable parameters

Equations (3.6) and (3.7) provide a set of constitutive equations for a nanocomposite melt. To describe distribution of meso-regions with various energies, we adopt the generalized random energy model with

$$f(v) = f_0 \exp\left[-\frac{1}{2}\left(\frac{v}{\sigma}\right)^\beta\right] \quad (v \geq 0), \quad f(v) = 0 \quad (v < 0), \quad (3.8)$$

where  $\beta$  and  $\sigma$  and positive coefficients, and the pre-factor  $f_0$  is found from the normalization condition.

Given a concentration of nanoclay  $\varphi$ , Eqs. (3.6)–(3.8) involve 4 material parameters: (i)  $\mu$  characterizes elastic properties of a nanocomposite melt, (ii)  $\gamma$  describes its viscoelastic response, (iii)  $\sigma$  reflects heterogeneity of the network, and (iv)  $\beta$  accounts for deviation of the distribution function from the Gaussian ansatz.

To describe the effect of nanoclay on material parameters, we postulate that (i) the rate  $\gamma$  is independent of  $\varphi$ , and (ii) the quantities  $\mu$ ,  $\beta$ , and  $\sigma$  change linearly with concentration of filler

$$\mu = \mu_0 + \mu_1\varphi, \quad \beta = \beta_0 + \beta_1\varphi, \quad \sigma = \sigma_0 + \sigma_1\varphi, \quad (3.9)$$

where  $\mu_m$ ,  $\beta_m$ , and  $\sigma_m$  ( $m = 0, 1$ ) are constants.

### 3.2. Simple shear

At simple shear with small strains, the strain tensor for macro-deformation reads  $\hat{\epsilon}(t) = \epsilon(t)\mathbf{e}_1\mathbf{e}_2$ , where  $\epsilon(t)$  stands for shear, and  $\mathbf{e}_m$  ( $m = 1, 2, 3$ ) are basic vectors of some Cartesian coordinate frame. The strain tensor for elastic deformations is presented in the form  $\hat{\epsilon}_e(t, v) = \epsilon_e(t, v)\mathbf{e}_1\mathbf{e}_2$ , where  $\epsilon_e(t, v)$  is a function to be found. Equations (3.1) and (3.7) result in the differential equation

$$\frac{\partial \epsilon_e}{\partial t}(t, v) + \gamma \exp(-v)\epsilon_e(t, v) = \frac{d\epsilon}{dt}(t), \quad \epsilon_e(0, v) = 0. \quad (3.10)$$

It follows from Eq. (3.6) that the shear stress  $\Sigma$  reads

$$\Sigma(t) = \mu \int_0^\infty \epsilon_e(t, v) f(v) dv. \quad (3.11)$$

To find the storage and loss moduli, we set

$$\epsilon(t) = \epsilon_0 \exp(i\omega t), \quad (3.12)$$

where  $\epsilon_0$  stands for amplitude,  $\omega$  denotes angular frequency of oscillations, and  $i = \sqrt{-1}$ . We search a steady-state solution of Eq. (3.10) in the form

$$\epsilon_e(t, v) = \epsilon_{e0} \exp(i\omega t), \quad (3.13)$$

where  $\epsilon_{e0}$  is an unknown coefficient. Combination of Eqs. (3.10), (3.12), and (3.13) yields  $\epsilon_{e0} = i\epsilon_0\omega(\gamma \exp(-v) + i\omega)^{-1}$ . It follows from this relation and Eqs. (3.11)–(3.13) that

$$\Sigma(t) = \mu\epsilon(t) \int_0^\infty \frac{i\omega}{\gamma \exp(-v) + i\omega} f(v) dv.$$

Introducing the notation  $\Sigma(t)/\epsilon(t) = G'(\omega) + iG''(\omega)$ , we find that

$$\begin{aligned} G'(\omega) &= \mu \int_0^\infty \frac{\omega^2}{\gamma^2 \exp(-2v) + \omega^2} f(v) dv, \\ G''(\omega) &= \mu \int_0^\infty \frac{\gamma \omega \exp(-v)}{\gamma^2 \exp(-2v) + \omega^2} f(v) dv. \end{aligned}$$

## 4. Fitting of observations

To find adjustable parameters in Eqs. (3.8) and (3.14), we approximate the experimental data depicted in Figures 1–4. Each set of observations for the storage modulus  $G'(\omega)$  and loss modulus  $G''(\omega)$  is matched separately. For each polymer matrix, we begin with approximation of observations on a nanocomposite melt with  $\varphi = 5$  wt.-%. To determine the best-fit parameters  $\mu$ ,  $\beta$ ,  $\gamma$ , and  $\sigma$ , we fix some intervals  $[0, \beta_{\max}]$ ,  $[0, \gamma_{\max}]$ , and  $[0, \sigma_{\max}]$ , where the quantities  $\beta$ ,  $\gamma$ , and  $\sigma$  are assumed to be located, and divide these











